



Basic ingredients for mathematical modeling of tumor growth *in vitro*: Cooperative effects and search for space

F.H.S. Costa^{a,*}, M. Campos^b, O.E. Aiello^c, M.A.A. da Silva^d

^a Departamento de Física, FFCLRP, Universidade de São Paulo, 14040-901 Ribeirão Preto, São Paulo, Brazil

^b Departamento de Química e Ciências Ambientais, IBILCE, Universidade Estadual Paulista Júlio de Mesquita Filho, 15054-000 São José do Rio Preto, São Paulo, Brazil

^c Departamento de Física Médica, UNIFEB, 14783-226 Barretos, São Paulo, Brazil

^d Departamento de Física e Química, FCFRP, Universidade de São Paulo, 14040-903 Ribeirão Preto, São Paulo, Brazil

AUTHOR HIGHLIGHTS

- We show that a basic requirement to simulate successfully the tumor growing *in vitro* is to adopt a sigmoidal growth rate.
- We use a different kind of dynamical Monte Carlo method, building the waiting times along the simulation.
- We have obtained non-Poissonian distributions for these waiting times.

ARTICLE INFO

Article history:

Received 11 February 2013

Received in revised form

21 June 2013

Accepted 31 July 2013

Available online 14 August 2013

Keywords:

Tumor growth

Dynamical Monte Carlo

Mathematical modeling

ABSTRACT

Based on the literature data from HT-29 cell monolayers, we develop a model for its growth, analogous to an epidemic model, mixing *local* and *global* interactions. First, we propose and solve a deterministic equation for the progress of these colonies. Thus, we add a stochastic (local) interaction and simulate the evolution of an Eden-like aggregate by using dynamical Monte Carlo methods. The growth curves of both deterministic and stochastic models are in excellent agreement with the experimental observations. The waiting times distributions, generated via our stochastic model, allowed us to analyze the role of mesoscopic events. We obtain log-normal distributions in the initial stages of the growth and Gaussians at long times. We interpret these outcomes in the light of cellular division events: in the early stages, the phenomena are dependent each other in a multiplicative geometric-based process, and they are independent at long times. We conclude that the main ingredients for a good minimalist model of tumor growth, at mesoscopic level, are intrinsic cooperative mechanisms and competitive search for space.

© 2013 Elsevier Ltd. All rights reserved.

1. Introduction

Mathematical modeling of biological systems, such as tumor growth, has an important role on *in vitro* (or *in vivo*) experiments concerning to formulate hypotheses about mechanisms and in suggesting new assays (Byrne, 2010). In fact, there is a growing interest in cancer modeling, since the scientific community begins to see it as a complex systems disease (Hornberg et al., 2006; Laubenbacher et al., 2009), which involves from genetic alterations (Hanahan and Weinberg, 2000) up to tissue aspects (Titz and Jeraj, 2008; Rejniak and McCawley, 2010). Regarding to clinical applications, one believes that the integration of imaging, treatment-response relationships, molecular basis, and predictive trials might

speed up the development of more specific and more effective therapies (Byrne, 2010; Laubenbacher et al., 2009; Stewart and Li, 2007; Titz and Jeraj, 2008; Barazzuol et al., 2010; Kazmi et al., 2012; Román-Romaán and Torrez-Ruiz, 2012). Thus, we emphasize the importance of both mathematical and biological modeling and their uses in a complementary way (Byrne, 2010).

Tumor evolution is a complex process involving several phenomena at different scales (Preziosi, 2003). An approach for the growth may be done looking at mesoscopic events; e.g., cell–cell and cell–environment interactions, time interval between duplications, competition for space, formation or break of bonds that maintain the aggregate structure, and the temporal dynamics of the colonies size. To simulate such tumor progress, we may construct simple models just representing cells by its physical properties, despite their biological complexity (Drasdo et al., 2007). An important contribution of such systematizations (Block et al., 2007; Huergo et al., 2012), even if in two dimensions, is the classification of tumor growth patterns (Guiot et al., 2003),

* Corresponding author. Tel.: +55 1636024840.

E-mail addresses: fhsantanacosta@gmail.com, fhscosta@usp.br (F.H.S. Costa), maasilva@fcrp.br (M.A.A. da Silva).

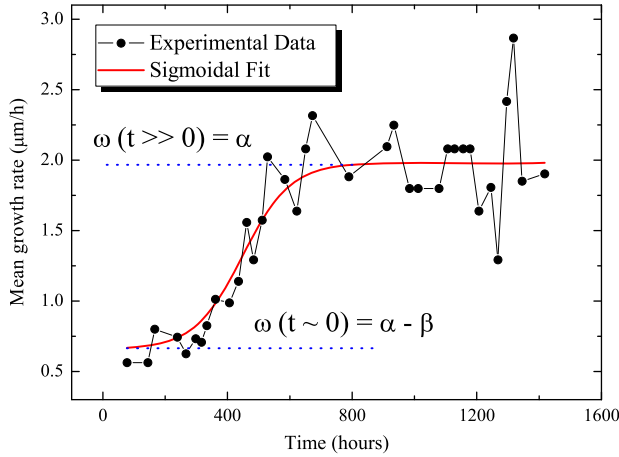


Fig. 1. The growth rate of the mean radius of aggregates of HT-29 cells (Brú et al., 2003). The blue dotted lines show the initial rate and its saturation. (For interpretation of the references to color in this figure caption, the reader is referred to the web version of this article.)

by generic mechanisms at individual cell level (migration, division, etc.), including molecular inter and intracellular regulation effects (Jiang et al., 2005), pressure effects (Brú and Casero, 2006) and evolution of cooperation (Alexrod et al., 2006). Also, one could use these models to identify cellular activities, which modified, would result in a maximal inhibition of multicellular evolution, and thus, point out potential therapeutic targets (Block et al., 2007; Katira et al., 2012). Brú and colleagues (Brú et al., 1998, 2003), in their investigation of pattern formation from several cell lines, highlighted the importance of the geometric structure and competition for space on the aggregate boundary. In recent work (Radszwejt et al., 2009), the authors search for simple and common mechanisms for tumor growth; through analysis of 2D and 3D models they suggested that single cell-based models in two-dimensions may describe well the general dynamics of its population.

In the search of mechanisms for tumor growth, by using simple models, we raised the following question: what ingredients are necessary to capture important features of tumor kinetics in the mesoscopic scale? Our belief is that cooperative effects and competitive search for space is the answer. In the next section we present the numerical method and the model used to simulate tumor growth; results and discussion appear within the third section, and in the last one we show the conclusions and point out our perspectives for future works.

2. Model and methods

We start our modeling approach, in the continuous limit, by fitting the experimental data (see Fig. 1) by using the following sigmoidal equation:

$$\omega(t) = \alpha - \frac{\beta}{1 + \exp[\gamma(t - t_c)]}, \quad (1)$$

with $\omega(t) \equiv dr(t)/dt$ being the mean radius rate.¹ At early times the growth rate is lower, constant, and given by $\omega_0 = \alpha - \beta$. After a critical time t_c , the curve changes its behavior by going to another constant value (α). The parameter γ determines how fast the rate changes from $\alpha - \beta$ to α ($\alpha > \beta$). Thus, given the condition $r(0) = r_0$,

we can find the equation to the mean radius:

$$r(t) = r_0 + \frac{\beta}{\gamma} \ln \left\{ \frac{\exp[-\gamma(t - t_c)] + 1}{\exp(\gamma t_c) + 1} \right\} + \alpha t. \quad (2)$$

Now, we introduce a discrete (minimalist) model using a lattice with $M = L \times L$ sites, in which each site can only be in a tumor status T or in an empty status V . We assume that the occupancy probability (p_0) of an empty site next to a tumor site carries the local and global information of the system at each instant; our global/local interaction is different from the one in the literature for epidemic models (Aiello et al., 2000; Aiello and da Silva, 2003; Cardy and Grassberger, 1985). There, they put the effects explicitly, while here, we bring them together. In this context, we assume that p_0 comes directly from Eq. (1) by doing $p_0 = p_0(t) \equiv \omega(t)/\alpha$; consequently, we can write the transition rate for each empty site in the form $g_q(t) \propto [1 - (1 - p_0)^{\eta_q}]$ (Cardy and Grassberger, 1985), where η_q is the number of neighbors with status T of an empty site labeled with index q . Finally, we can write the transition probability per unit of time as

$$g_q(t) = b \left\{ 1 - \left[\left(\frac{\beta}{\alpha} \right) \frac{1}{1 + \exp[\gamma(t - t_c)]} \right]^{\eta_q} \right\}, \quad (3)$$

where b is the frequency of new tumor sites in a colony. Here we consider the first and second nearest neighbors, i.e., $0 \leq \eta_q \leq 8$. Also we consider that just one event occurs at each time interval Δt , i.e., $|\Delta n_T| = |\Delta n_V| = 1$. Thus, we can write the stochastic equation (Aiello and da Silva, 2003)

$$\frac{d}{dt} n_T(t) = \sum_j \langle g(t) \rangle_j P_j(t) n_0^j, \quad (4)$$

where $\sum_j(\dots)$ is the sum of over all possible system configurations available at time t ; $\langle g(t) \rangle_j = \sum_q g_q^j(t)/n_0^j$ represents the mesoscopic rate of the growth (an average over each configuration j); $P_j(t)$ is the probability of finding the system in the state j at time t ; and n_0 (from now on we will omit the configurational index j for all variables) is the total number of empty sites in the colony-medium interface; some of these sites may be inside the colony. The total number of lattice sites is $M = n_T + n_V$, being $n_V = n_0 + \tilde{n}_V$ the total number of empty sites, i.e., those (n_0) which contribute to the increase of n_T (with $\eta_q > 0$), plus those (\tilde{n}_V) that do not contribute (with $\eta_q = 0$). We neglect (explicitly) the cell death, migration and other process that could reduce the aggregate area, i.e., the transition $T \rightarrow V$.

We solve Eq. (4) using the dynamical Monte Carlo method (DMC) approach (Aiello and da Silva, 2003). In the simulations, we estimate the average waiting time between two events with the expression

$$\Delta t^{(n_T)} = \frac{1}{\sum_q g_q(t)}. \quad (5)$$

The superscript (n_T) denotes the average waiting time between the $(n_T - \Delta n_T)$ -th and the (n_T) -th *cell*² growth event. Finally, we use the following dynamical hierarchy (Aiello et al., 2000):

$$H_q = \frac{g_q(t)}{\max[g_q(t)]} = \frac{1 - (1 - p_0)^{\eta_q}}{1 - (1 - p_0)^{\eta_{\max}}}, \quad (6)$$

where $\max[g_q(t)]$ denotes the maximum value of $g_q(t)$.

Operationally, one does the DMC procedure by choosing a site of the set $\{n_0\}$ with equal probability, and then compares H_q with a random number ξ , uniformly distributed in the interval $[0, 1]$. If $H_q > \xi$, one accepts the new configuration and updates the

¹ The derivative is obtained from the average slopes of adjacent points for each experimental data point.

² The word *cell* (in italic) does not represent biological cells, but just the T sites; we believe that a rescale factor can make the direct correspondence between n_T and the actual number of cells (Jiang et al., 2005).

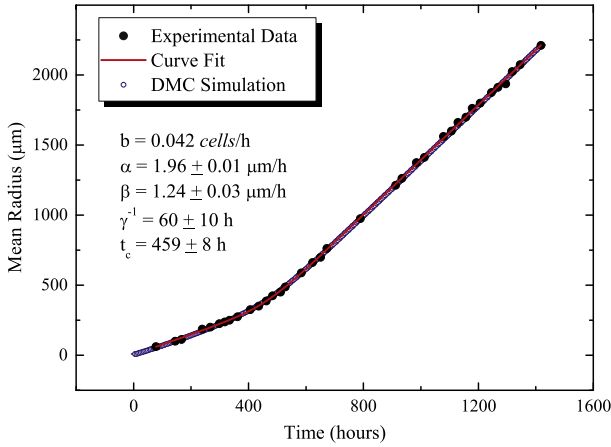


Fig. 2. Temporal evolution of the mean radius of aggregates of the HT-29 cell line. We can see the good agreement between the experimental data, analytical Eq. (2) and simulation.

time: $t \rightarrow t + \Delta t^{(nr)}$; n_T increases of Δn_T , another mean radius is found, and the mesoscopic rate is updated (see Appendix A to the implementation of the mean radius and mesoscopic rate calculus). On the other hand, if $H_q \leq \xi$, a new site is chosen and the process restart. At long times, we have $g_q(t) \rightarrow b$, giving $H_q = 1$; thus, the probability of transition will be the same of the Eden-A model (Jullien and Botet, 1985), i.e., $1/n_0$. For early times, the behavior is not the same, because $g_q(t)$ depends locally on the number of neighboring T -sites, so the chance of chooses and fill a site will be H_q/n_0 .

3. Results and discussion

The sigmoidal growth rate *ansatz* allowed us to obtain Eq. (2) for the mean radius. Adjusting it to experimental data, we could find the values of the parameters α , β , γ and t_c showed in Fig. 2. Eq. (1) points out three different regimes: the first one in which the growth rate is almost constant, equals to $\alpha - \beta$; a second one, a transition regime, and the last one, where the growth rate is constant with value α . Suppose that all cells are synchronized and duplicate simultaneously, thus, the time to form a new layer can be given by the product of the number of the empty sites by the waiting time. However, as this does not occur (the cells are not synchronized), we multiply this by the average probability of occupation of an empty site, i.e., $t_{\text{cycle}} = n_0 \Delta t^{(nr)} \langle H_q \rangle$. This results that the average cell cycle time is $1/b$. By adjusting the parameter b in the simulation to fit the experimental data we obtain $1/b \approx 23, 8$ h, what is a good value, near to the expected 24 h (Tonkinson et al., 1999; Calabro-Jones et al., 1982). We believe that the apparent sigmoidal shape of the experimental data showed in Fig. 1 may result from cooperative effects at the growing perimeter of the colony. A possible cooperative mechanism is that the cells do not grow immediately after being plated in culture bottles; they need to become adherent to the plate surface for proliferate, i.e., there is a critical nucleus stabilized by cohesive forces favoring the adhesion of the cells to the plate surface. However, this hypothesis needs to be experimentally checked yet.

For study of the stochastic model, we used a lattice of $L=500$ sites. The relation between the length of the lattice side L and the diameter of a cell may be given by $1/L \equiv d_0 = 10 \mu\text{m}$ (Drasdo and Hoëhne, 2005). Initially one places a single cell in the lattice center. In Figs. 2 and 4, one takes the sample average from 200 runs, with estimated errors of about 1%, which makes the error bars smaller than the symbols of the measured quantities. We built the distributions of the average waiting times with 10^6 trajectories. We choose

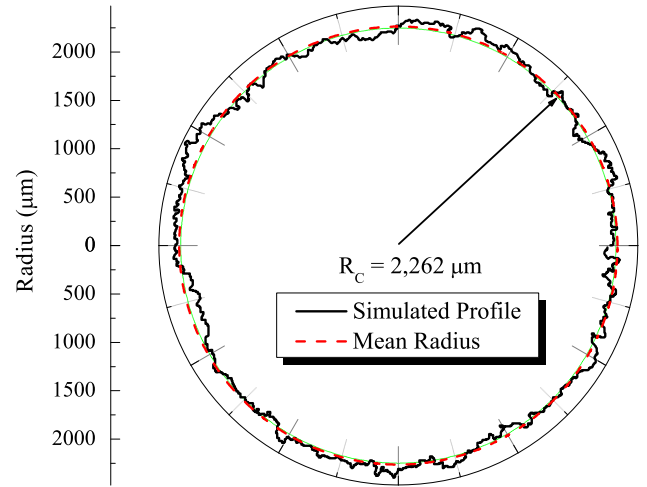


Fig. 3. Typical colony profile obtained in a simulation. Here $t \approx 1429$ h, $n_T = 155,551$ cells and $n_0 = 6509$ sites. Most of the empty sites, at this point, are in the colony border.

$\eta_{\max} = 8$ to calculate $\max[g_q(t)]$, since rapidly appears a hole in the colony. The number of cells required to appear the first empty site with $\eta_q = 8$ was about $n_T = 53$. Even updating η_{\max} at each generated configuration j , the results obtained for the growth curve were the same for $\eta_{\max} = 8$.

Fig. 2 shows the excellent agreement between the experimental data, its fitting using Eq. (2) and the DMC simulation. Thus, we believe that Eq. (3) represents the basic mechanism by which the empty sites are filled. The DMC procedure properly reproduces the events at the mesoscopic scale, making it a potential tool to further studies on tumor cell populations. One should note that the stochastic approach (Eq. (4)) reproduces a circular symmetry at long times, because $dn_T/dt = b \langle n_0 \rangle$, since $\omega(t)/\alpha \rightarrow 1$ in this limit. This agrees with the choices of $n_T \propto r^2$ and $n_0 \propto r$ (Brú et al., 1998). Notice that in Fig. 3 that these relations agree with the generated data. We cannot state the same for initial times, once $\langle g(t) \rangle$ becomes dependent on η_q in a intrincated way.

For comparison purposes with another MCD method (Aiello et al., 2000; Block et al., 2007; Radszuweit et al., 2009; Fichtorn and Weinberg, 1991), we get the waiting time from a Poisson distribution, estimating the time interval for each configuration j with $\Delta t_p^{(nr)} = -\ln(\xi_2)/\sum_q g_q(t)$. In the following, we do the same procedure described previously to compute the cell number and the mean radius. In Fig. 4a we see that both, the evaluation by a Poisson process and the estimate via Eq. (5), produce indistinguishable growth curves, since $\Delta t^{(nr)} = \langle \Delta t_p^{(nr)} \rangle$. However, one superimposes the approximation by a Poisson process (Fig. 4b), while through the methodology described in Aiello and da Silva (2003), one builds up the waiting time distribution during the simulation. We also do an iterative calculation of the temporal evolution (stochastic Euler method), with the approximation $r(t + \Delta t_e) \approx r(t) + \omega(t) \Delta t_e$, were $\Delta t_e = \{\max[g_q(t)] n_0\}^{-1}$. One expects the agreement with this method, because

$$\Delta t_e = \sum_q \left\{ \frac{g_q(t)}{\max[g_q(t)]} \right\} \left(\frac{1}{n_0} \right) \Delta t^{(nr)}. \quad (7)$$

The average waiting time distribution calculated through Eq. (5) yielded the data displayed in Fig. 5. Here we adjusted a curve $\rho_m = a_m \exp(-b_m [f_m(\tau)]^2)$. The subscript m represents the curves $m=g$, gaussian ($f_g = \tau - c_g$) and $m=l$, log-normal ($f_l = \ln(\tau) - \ln(c_l)$). The number of observations were normalized by its maximum and were plotted against $\tau = \Delta t^{(nr)}/\langle \Delta t^{(nr)} \rangle$. The adjusted parameters are in Table 1. We do not show the values a_m and c_m , because

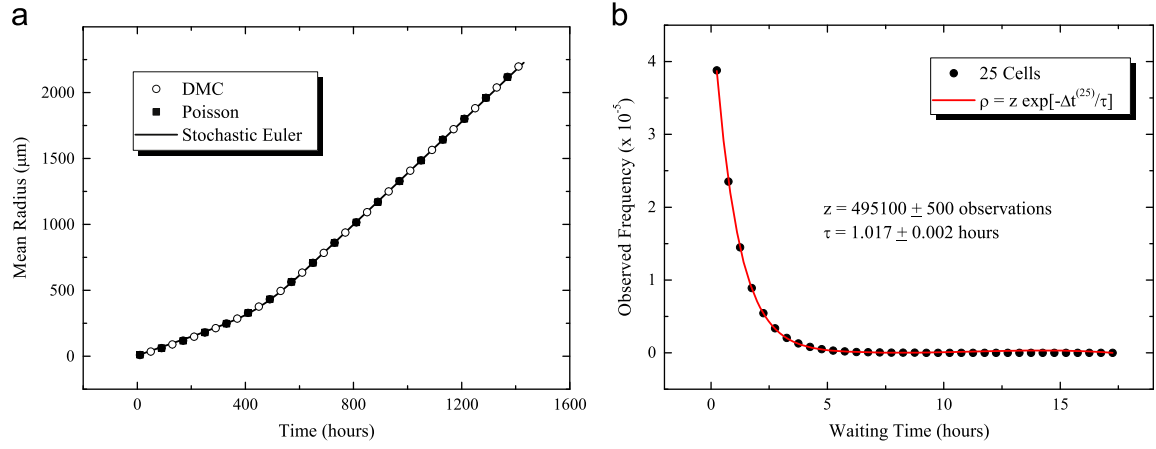


Fig. 4. (a) The mean radius $r(t)$ obtained with three different methods. (b) The Poissonian distribution of $\Delta t_p^{(25)}$. Despite the agreement of the DMC method for the mean radius calculus with the Poissonian method, we cannot expect that the system evolution follows a Poissonian process, because the events are correlated.

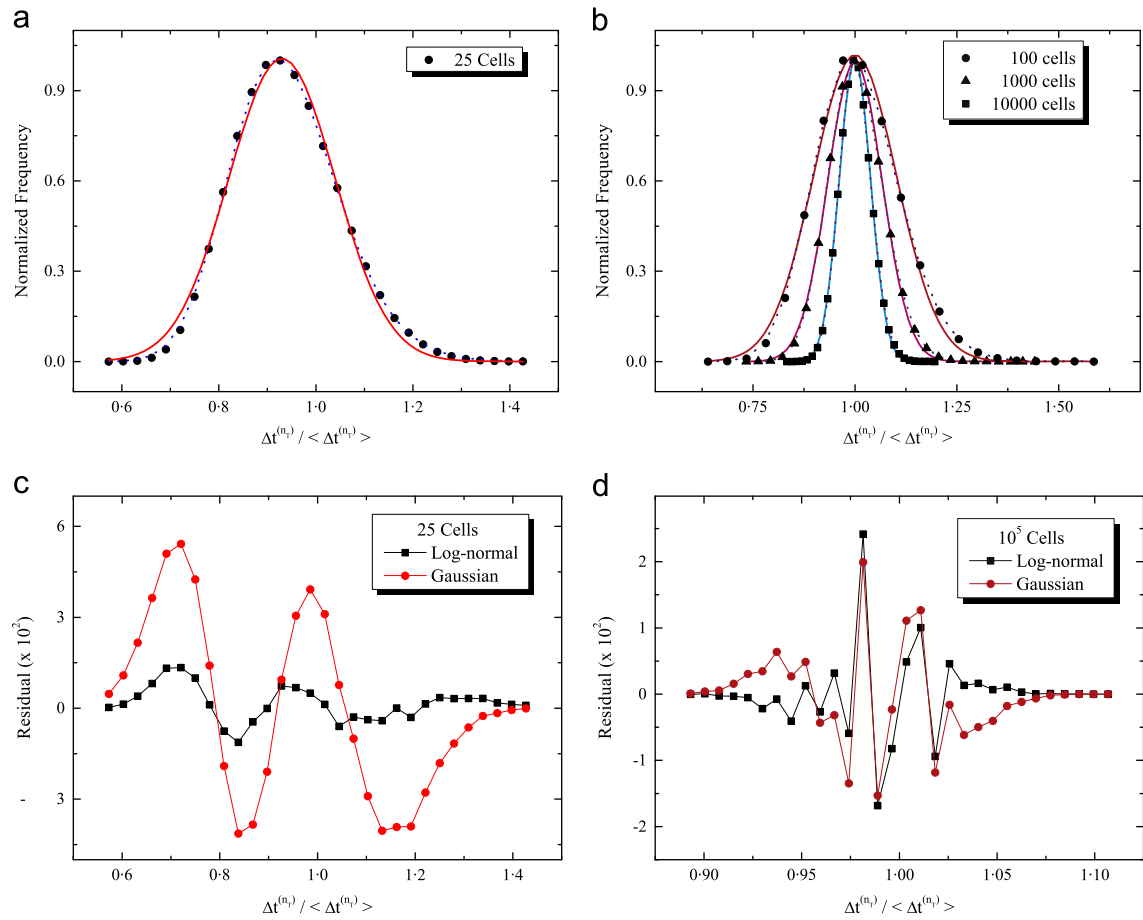


Fig. 5. The waiting time distribution for several n_T . (a) We have the Gaussian fit (solid lines) and the log-normal (dotted lines). (b) The normalized observed frequency plotted against $\Delta t^{(n_T)} / \langle \Delta t^{(n_T)} \rangle$. One can see that these curves are very close, but the most important feature, for this work, is that they are not Poissonian distributions. In (c) and (d) we show with a depth the better adjustment of the log-normal curve in the region of few cells; when the aggregate size becomes larger, the distributions are not distinguishable.

Table 1
The adjusted parameters to ρ_m .

Cells	25	10^2	10^3	10^4	10^5
b_g	42	48	114	340	974
b_l	35.7	47.8	113.9	339.5	947
$\langle \Delta t^{(n_T)} \rangle$	1.10	0.47	0.117	1.62×10^{-2}	4.56×10^{-3}

The errors are less than 1%.

$a_{g,l} \approx c_{g,l} \approx 1$. To see the difference between fits with more details, we show the residuals of ρ_g and ρ_l . With few cells, the log-normal curve were better, while in a big cluster, there is no much distinction between both.

Rigorously, for random processes having a Poisson distribution is required independence of events (Aiello et al., 2000; Aiello and da Silva, 2003; Fichtorn and Weinberg, 1991). Nevertheless, as seen before, log-normal and Gaussian curves fit well our data when using the average waiting times given by Eq. (5), reflecting

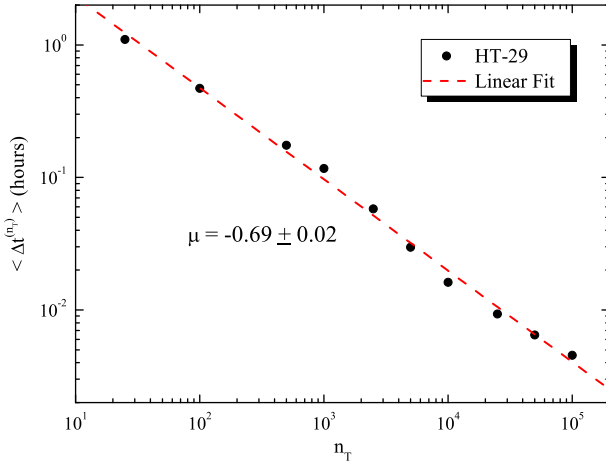


Fig. 6. A linear fit of $\log[\langle \Delta t^{(n_T)} \rangle]$ plotted against $\log(n_T)$ giving the μ parameter of the relation $\langle \Delta t^{(n_T)} \rangle \propto n_T^{-\mu}$.

that there may have some dependency among the events. When the colony has few cells, the behavior of $\Delta t^{(n_T)}$ depends on the empty site choice in a particular position, which may cause a log-normal process. This emphasizes the importance of the local interactions, at least in this initial stage. On the other hand, when the colony is large, the waiting time becomes proportional to the probability of choosing an empty site, this makes $\Delta t^{(n_T)}$ to depend negligibly on the position of the site chosen. However, we believe that geometric details with the local interactions of the system *in vitro* still have relevance in this region, especially to the fractality of the aggregate (Drasdo et al., 2007; Block et al., 2007; Brú et al., 1998, 2003). We could not reproduce the experimental fractal dimension with our simple model in which the local interactions effect vanishes to large clusters. Plotting the average of the log-normal distributions against each size (Fig. 6), we could find the relationship $\langle \Delta t^{(n_T)} \rangle \propto n_T^{-\mu}$, with $\mu = 0.69 \pm 0.02$.

4. Conclusions and Perspectives

In this work, we modeled the tumor growth *in vitro* using a mesoscopic approach. We evaluated its temporal dynamic by continuous equations and DMC simulations, being that all results agreed among themselves and with the experimental data.

Using the DMC procedure (Aiello and da Silva, 2003), we found non-Poissonian waiting times distributions, which are useful to study the behavior of tumoral colonies. We showed that both simulations, the Poissonian type and our approach, agreed. However, we note that the above discussed process cannot be truly Poissonian; it is just a numerical approach that gives the correct solution for the master equation (Aiello et al., 2000; Fichtorn and Weinberg, 1991). We built the distribution of waiting times for several values of n_T , and we adjusted these data with log-normal and Gaussian distributions, meaning that the events involved in the processes are in some way dependent; we observe that log-normal distribution, usually, fit better to our data than the Gaussian ones. We found that the average waiting time, decays with the number of cells given by the power law $\langle \Delta t^{(n_T)} \rangle \propto n_T^{-\mu}$. The value of the exponent μ may be an intrinsic feature of monolayer growth, but more detailed studies are necessary to clarify this result.

We believe that the basic mechanisms which make a minimalist model works for monolayer tumor growth *in vitro*, in the mesoscopic scale, are competitive search for empty spaces and intrinsic cooperative mechanisms. These cooperative mechanisms may be correlated with several factors, such as nutrients consumption and

adhesive/cohesive forces. In future work, we intend to do investigations *in vitro* to see how the number of cells varies with the mean radius of the colonies. We, also, intend to verify experimentally the lognormality of the waiting time distributions, and extend our model to include cell deformation, cell cycle, nutrients and adhesion/cohesion effects; we expect to reproduce naturally the sigmoidal rate behavior with these additional ingredients.

Acknowledgments

F.H.S.C. is grateful to funding support from CAPES and we thank FAPESP (Grant no. 2012/03823-5) for financial assistance.

Appendix A. The mean radius and growth rate calculation

Along the system evolution, we are interested in the mean radius calculation, given by $\langle r \rangle = \sqrt{2}d_0r_g$, where d_0 is the cell diameter, and r_g is the gyration radius, $r_g = \sqrt{(1/n_T) \sum_{T=1}^{n_T} [\mathbf{r}_T - \mathbf{r}_{cm}(t)]^2}$, being n_T the cell number, \mathbf{r}_T the cell localization in the lattice, and $\mathbf{r}_{cm}(t) = (1/n_T) \sum_{T=1}^{n_T} \mathbf{r}_T$, the center of mass. We define the quantity $S(t) \equiv \sum_{T=1}^{n_T} [\mathbf{r}_T - \mathbf{r}_{cm}(t)]^2$ to use below. When the system increases by just one cell in the time interval $\Delta t^{(n_T)} = \Delta t$, i.e., $n_T \rightarrow n_T + 1$, we can calculate a quantity δ defined by

$$\delta \equiv \Delta \mathbf{r}_{cm} = \mathbf{r}_{cm}(t) - \mathbf{r}_{cm}(t - \Delta t). \quad (\text{A.1})$$

To optimize the calculus of r_g , instead of sweep all T -sites, we will consider a function $S'(t)$ given by

$$S'(t) = S(t - \Delta t) + [\mathbf{r}_{n_T} - \mathbf{r}_{cm}(t)]^2. \quad (\text{A.2})$$

In this context, $S(t - \Delta t) = \sum_{T=1}^{(n_T-1)} [\mathbf{r}_T - \mathbf{r}_{cm}(t - \Delta t)]^2$. Using Eq. (A.1) one can rewrite Eq. (A.2) as

$$S'(t) = \sum_{T=1}^{n_T-1} [\mathbf{r}_T - [\mathbf{r}_{cm}(t) - \delta]]^2 + [\mathbf{r}_{n_T} - \mathbf{r}_{cm}(t)]^2. \quad (\text{A.3})$$

After some algebraic manipulation we get

$$S'(t) = \sum_{T=1}^{n_T-1} [\mathbf{r}_T - \mathbf{r}_{cm}(t)]^2 + [\mathbf{r}_{n_T} - \mathbf{r}_{cm}(t)]^2 + 2\delta \cdot \sum_{T=1}^{n_T-1} [\mathbf{r}_T - \mathbf{r}_{cm}(t)] + \sum_{T=1}^{n_T-1} \delta^2. \quad (\text{A.4})$$

Considering that

$$\sum_{T=1}^{n_T-1} [\mathbf{r}_T - \mathbf{r}_{cm}(t)]^2 + [\mathbf{r}_{n_T} - \mathbf{r}_{cm}(t)]^2 = \sum_{T=1}^{n_T} [\mathbf{r}_T - \mathbf{r}_{cm}(t)]^2 = S(t), \quad (\text{A.5})$$

and, as by definition $\sum_{T=1}^{n_T} [\mathbf{r}_T - \mathbf{r}_{cm}(t)] = 0$, we obtain an alternative form to $S(t)$ from Eq. (A.4):

$$S(t) = S'(t) + 2\delta \cdot [\mathbf{r}_{n_T} - \mathbf{r}_{cm}(t)] - \delta^2(n_T - 1). \quad (\text{A.6})$$

This equation is useful due to the gain in CPU time, since we do not need to sweep all T -sites at each update, as expected in r_g definition; we can use just the current value of n_T to update r_g .

Also in order of optimize the CPU time, in the waiting time estimation (Eq. (5)) the growth rate can be replaced by

$$\sum_q g_q(t) = \sum_{\eta=1}^{\eta_{\max}} n_{\eta} [1 - (1 - p_0)^{\eta}], \quad (\text{A.7})$$

being n_{η} the number of empty sites with η tumoral neighbors. Note that $\sum_{\eta=1}^{\eta_{\max}} n_{\eta} = n_0$; this relation is important when $p_0 \rightarrow 1$. In this way, the update is simplified sweeping only η_{\max} elements, instead of sweep all the q elements to find the growth rate.

References

- Aiello, O.E., da Silva, M.A.A., 2003. New approach to dynamical Monte Carlo methods: application to an epidemic model. *Physica A* 327, 525–534.
- Aiello, O.E., Hass, V.J., daSilva, M.A.A., Caliri, A., 2000. Solution of deterministic-stochastic epidemic models by dynamical Monte Carlo method. *Physica A* 282, 546–558.
- Alexrod, R., Alexrod, D.E., Pienta, K.J., 2006. Evolution of cooperation among tumor cells. *Proceedings of National Academy of Sciences* 103 (36), 13474–13479.
- Barazzuol, L., Burnet, N.G., Jena, R., Jones, B., Jefferies, S.J., Kirkby, N.F., 2010. A mathematical model of brain tumour response to radiotherapy and chemotherapy considering radiobiological aspects. *Journal of Theoretical Biology* 262, 553–565.
- Block, M., Schöll, E., Drasdo, D., 2007. Classifying the expansion kinetics and critical surface dynamics of growing cell populations. *Physical Review Letters* 99, 248101.
- Brú, A., Albertos, S., Subiza, J.L., García-Asenjo, J.L., Brú, I., 2003. The universal dynamics of tumor growth. *Biophysics Journal* 85, 2948–2961.
- Brú, A., Casero, D., 2006. The effect of pressure on the growth of tumour cell colonies. *Journal of Theoretical Biology* 243, 171–180.
- Brú, A., Pastor, J.M., Fernaud, I., Brú, I., Melle, S., Berenguer, C., 1998. Super-rough dynamics of tumor growth. *Physical Review Letters* 81 (18), 4008–4011.
- Byrne, H.M., 2010. Dissecting cancer through mathematics: from the cell to the animal model. *Nature Reviews Cancer* 10, 221–230.
- Calabro-Jones, P.M., Byfield, J.E., Ward, J.F., Sharp, T.R., 1982. Time-dose relationships for 5-fluorouracil cytotoxicity against human epithelial cancer cells *in vitro*. *Cancer Research* 42, 4413–4420.
- Cardy, J.L., Grassberger, P., 1985. Epidemic models and percolation. *Journal of Physics A – Mathematical and General* 18, L267–L271.
- Drasdo, D., Hoehme, S., 2005. A single-cell-based model of tumor growth *in vitro*: monolayers and spheroids. *Physical Biology* 2, 133–147.
- Drasdo, D., Hoehme, S., Bloch, M., 2007. On the role of physics in the growth pattern formation of multi-cellular systems: what we can learn from individual-cell based models? *Journal of Statistical Physics* 128 (1/2), 287–345.
- Fichtorn, K.W., Weinberg, W.H., 1991. Theoretical foundations of dynamical Monte Carlo simulations. *Journal of Chemical Physics* 95 (2), 1090–1096.
- Guiot, C., Degiorgis, P.G., Delsanto, P.P., Gabriele, P., SDeisboeck, T., 2003. Does tumor growth follow a “universal law”? *Journal of Theoretical Biology* 225, 147–151.
- Hanahan, D., Weinberg, R.A., 2000. The hallmarks of cancer. *Cell* 100, 57–70.
- Hornberg, J.J., Bruggeman, F.J., Westerhoff, H.V., Lankelma, J., 2006. Cancer: a systems biology disease. *Biosystems* 83, 81–90.
- Huergo, M.A.C., Pasquale, M.A., Gonzalez, P.H., Bolzán, A.E., Arvia, A.J., 2012. Growth dynamics of cancer cells colonies and their comparison with noncancerous cells. *Physical Review E* 85, 011918.
- Jiang, Y., Pjesivac-Grbovic, J., Cantrell, C., Freyer, J.P., 2005. A multiscale model for avascular tumor growth. *Biophysics Journal* 89, 3884–3894.
- Jullien, R., Botet, R., 1985. Scaling properties of the surface of the Eden model in $d=2, 3, 4$. *Journal of Physics A – Mathematical and General* 18, 2279–2287.
- Katira, P., Zaman, M.H., Bonnacaze, R.T., 2012. How changes in cell mechanical properties induce cancerous behavior. *Physical Review Letters* 108, 028103.
- Kazmi, N., Hossain, M.A., Phillips, R.M., Al-Manun, M.A., Bass, R., 2012. Avascular tumour growth dynamics and the constraints of protein binding for drug transportation. *Journal of Theoretical Biology* 313, 142–152.
- Laubenbacher, R., Hower, V., Jarrah, A., Torti, S.V., Shulaev, V., Mendes, P., Torti, F.M., Akman, S., 2009. A system biology view of cancer. *BBA-Reviews Cancer* 1796, 129–139.
- Preziosi, L., 2003. *Cancer Modelling and Simulation*. CRC Press, Boca Raton.
- Radszuweit, M., Block, M., Hengstler, J.G., Schöll, E., Drasdo, D., 2009. Comparing the growth kinetics of cell populations in two and three dimensions. *Physical Review E* 79, 051907.
- Rejniak, K.A., McCawley, L.J., 2010. Current trends in mathematical modeling of tumor–microenvironment interactions: a survey of tools and applications. *Experimental Biology and Medicine* 235, 411–423.
- Román-Romaán, P., Torrez-Ruiz, F., 2012. Inferring the effect of therapies on tumor growth by using diffusion processes. *Journal of Theoretical Biology* 314, 34–56.
- Stewart, R.D., Li, X.A., 2007. BRGT: biologically guided radiation therapy—the future is fast approaching!. *Medical Physics* 34, 3739–3751.
- Titz, B., Jeraj, R., 2008. An imaging-based tumour growth and treatment response model: investigating the effect of tumour oxygenation on radiation therapy response. *Physics in Medicine and Biology* 53, 4471–4488.
- Tonkinson, J.L., Worzalla, J.F., Teng, C.H., Mendelsohn, L.G., 1999. Cell cycle modulation by a multitargeted antifolate, LY231514, increases in the cytotoxicity and antitumor activity of gencitabine in HT29 colon carcinoma. *Cancer Research* 59, 3671–3676.